THE ASTROPHYSICAL JOURNAL, 328:763–776, 1988 May 15

NEUTRAL STELLAR WINDS THAT DRIVE BIPOLAR OUTFLOWS IN LOW-MASS PROTOSTARS

SUSANA LIZANO AND CARL HEILES
Astronomy Department, University of California at Berkeley
LUIS F. RODRÍGUEZ
Universidad Nacional Autónoma de México
BON-CHUL KOO AND FRANK H. SHU
Astronomy Department, University of California at Berkeley
T. HASEGAWA AND S. HAYASHI
Nobeyama Radio Observatory
AND
I. F. MIRABEL
University of Puerto Rico
Received 1987 July 27; accepted 1987 November 2

ABSTRACT

Using the Arecibo radio telescope at the 21 cm line of atomic hydrogen, we detected a neutral *atomic* wind in the bipolar flow source HH 7–11. The H I gas reaches velocities up to ~ 170 km s^{-1} and has an associated mass-loss rate from the protostar of $\dot{M}_a \approx 3 \times 10^{-6}\ M_\odot\ \mathrm{yr}^{-1}$, which suffices to drive the observed CO bipolar flow. The 21 cm line profile indicates the H I wind to be decelerating, either as a function of increasing angle away from the central axis of the flow, or of increasing distance along that axis. The deceleration of the atomic wind may arise from interaction with the surrounding molecular cloud. Evidence exists that ambient molecular material has been entrained in the decelerating H I wind. At the Nobeyama 45 m telescope we detected HCO^+ at velocities intermediate between the H I wind and the CO bipolar outflow. The molecular gas associated with the HCO^+ (observed with a much smaller beam than the H I gas) has a total momentum flux 20–80 times greater than required to drive the extended CO gas *if* the relative abundances of HCO^+ and CO have their normal interstellar values. We deduce, therefore, that the HCO^+ abundance has been greatly enhanced in the regions of interaction of the atomic wind with the ambient cloud. Results obtained on the 12 m dish at NRAO Kitt Peak for the relative line intensities of HCO^+ and CO at low and intermediate velocities reinforce this conclusion. The Kitt Peak CO result is especially interesting because, in addition to a low-velocity line core plus a sloping intermediate-velocity line wing, the line spectrum shows another component, one with a roughly *rectangular* profile, which may represent the stellar wind itself before much interaction with the surrounding gas has taken place. From the ratio of line strengths of the high-velocity CO and H I, we deduce that a significant fraction of the available carbon atoms in the original stellar wind, perhaps all of them, is contained in the form of CO.

We also discuss more ambiguous evidence in H I and in OH for a decelerating neutral stellar wind from L1551 IRS 5. If the data are interpreted in an optimistic light, they imply the presence of an atomic wind roughly sufficient to account for the bipolar CO flow and the excess extended far-infrared radiation. In particular, both the *integrated* momentum and *instantaneous* energy requirements may be fulfilled by the marginally detected stellar wind in this source.

Subject headings: interstellar: molecules — radio sources: 21 cm radiation — stars: pre–main-sequence — stars: winds

I. INTRODUCTION

The detection of the stellar winds that power the CO outflows associated with young stellar objects (YSOs) in molecular clouds has become one of the urgent problems in the field of star formation. Very little is known about the physical conditions of these winds. Rodríguez and Cantó (1983) tried to detect the radio continuum signature of ionized winds from several bipolar sources. They found very low upper limits which suggested that the stellar winds, if present, may be largely neutral. Snell *et al.* (1985) found that the mass-loss rate $\dot{M}_i$ of ionized gas in L1551 IRS 5 was too low to drive the CO lobes. Strom *et al.* (1986) reached a similar conclusion by comparing the momentum input from the ionized component of the optical outflows (the so-called optical jets) with the momentum estimated for the molecular outflows in several sources that show both phenomena. For these sources, the wind or jet momentum injection is usually less than 10% of that needed to drive the observed CO outflows (see the reviews of Lada 1985 and Levreault 1985).

The failure to detect ionized stellar winds with sufficient power to drive CO bipolar outflows has motivated an unorthodox proposal for their origin in very large and rapidly rotating protostars (Hartmann and MacGregor 1982). This proposal involves a promising mechanism (centrifugally driven magnetic winds), but the specific objects discussed, if thermally supported in their interiors, would have untenably short

Kelvin-Helmholtz contraction times and, if centrifugally supported, would become massive disks. The latter line of investigation—very large and massive interstellar disks—was considered by Pudritz and Norman (1983, 1986) and by Uchida and Shibata (1985), but such theories lack a firm observational foundation (see, e.g., Walmsley and Menten 1987; Shu, Adams, and Lizano 1987).

Recent observations of extended far-infrared emission associated with the CO lobes of L1551 IRS 5 (Clark and Laureijs 1986; Edwards *et al.* 1986; Clark *et al.* 1986) suggest that there must be a powerful source of missing mechanical luminosity coming from a conventional protostar. (The stellar photons are judged insufficient to heat the very extended distribution of warm dust.) Thus, the direct measurement of a neutral stellar wind in this and other bipolar flow sources would help to clear up several related mysteries. In our own search, we were encouraged by Bally and Stark's (1983) discovery of high-velocity H I associated with outflows in NGC 2071; an alternative interpretation for this atomic hydrogen to the one offered in their paper (shock dissociation of H_2) is the possibility of a neutral stellar wind. In particular, Snell *et al.* (1984) calculated that the 0.1 $M_\odot$ of high-velocity atomic gas found by Bally and Stark suffices to power the observed CO flow in this source (but see Bally 1987).

II. OBSERVATIONS

Our primary observing objective was to use the high sensitivity of the Arecibo[1] telescope to try to detect weak broad lines of H I emission in a number of nearby bipolar flow sources (see Table 1 for a source list). The search succeeded unambiguously in the case of HH 7–11, which spawned two related proposals to use the Nobeyama[2] 45 m telescope and the NRAO[3] 12 m dish at Kitt Peak to search for associated high-velocity wings in a number of molecular species at millimeter wavelengths. Again, we found very interesting results, the interpretation of which meshed well (see § III) with the picture that we were developing to explain the H I observations. The observational procedures used in the molecular-line work will be discussed in § II*c*.

At Arecibo, we used the dual polarized 21 cm line feed with its associated electronics. Arecibo's 2048 channel correlation spectrometer was split into two 1024 channel banks, one for each polarization. Observations were performed by position switching every minute, i.e., by obtaining a reference spectrum on a nearby "off" position offset in various directions by a small angular increment, typically 10′. A crucial part of the technique was maintaining a fixed, unchanged local oscillator setting throughout long integrations; this allowed us to obtain a very flat baseline, without which we could not have detected a weak broad line. (For S255, which is a point continuum source, the resultant baseline is not flat because of frequency structure in the gain of the line feed.) Two examples of our results are shown in Figure 1: in HH 7–11 where we detected the sought-for signal, and AFGL 961 where we did not. The results in Figure 1 have undergone no processing other than the subtraction of "on" and "off" spectra (divided by the "off" spectrum and multiplied by the average system temperature of the "off" position). In particular, *no* "baseline fitting" has been performed. The procedure produces accurate source line-profiles except for frequencies (in the line core) where the reference position also has an antenna temperature that is a significant fraction of the system temperature. This underestimates the antenna temperature by no more than a factor of 2 for absolute velocities less than 20 km s^{-1}. Thus, the *intrinsic* flatness of our position-switched spectra provides confidence in the reality of our detection of a high-velocity atomic wind in HH 7–11 and in the quality of the null result for AFGL 961.

III. RESULTS AND INTERPRETATION FOR HH 7–11

Since clear and unambiguous evidence of high velocity H I was detected only in HH 7–11, we will discuss our results for this object first. HH 7–11 lies in the NGC 1333 region, in a molecular cloud with radial velocity v_{LSR} = 8.2 km s^{-1} (Lada *et al.* 1974; Ho and Barret 1980; Rudolph and Welch 1988). A string of blueshifted Herbig-Haro objects, HH 7–11, are aligned along the axis of the blueshifted lobe of a bipolar CO outflow (Snell and Ewards 1981), which is itself driven by the central infrared source SVS 13 (Strom, Vrba, and Strom, 1976).

[1] The Arecibo Observatory is part of the National Astronomy and Ionosphere Center, which is operated by Cornell University under contract with the National Science Foundation.

[2] NRO, a branch of the Tokyo Astronomical Observatory, University of Tokyo, is a cosmic radio observing facility open to outside users.

[3] The National Radio Astronomy Observatory is operated by Associated Universities, Inc., under contract with the National Science Foundation.

TABLE 1

LIST OF SOURCES OBSERVED AT ARECIBO

Source	α(1950)	δ(1950)	Observing Time (minutes)	Offset (10′)
HH 7–11	$03^h25^m58^s.2$	31°05′46″	76	north
			88	south
			88	east
			90	west
			45	parallel to bipolar axis
L1551 IRS 5	04 28 40.0	18 01 42	48	north
			48	east
			54	west
S255	06 09 59.0	18 00 15	44	north
			36	south
			48	east
			42	west
AFGL 961	06 31 59.0	04 15 09	18	north
			18	south
			22	east
			20	west

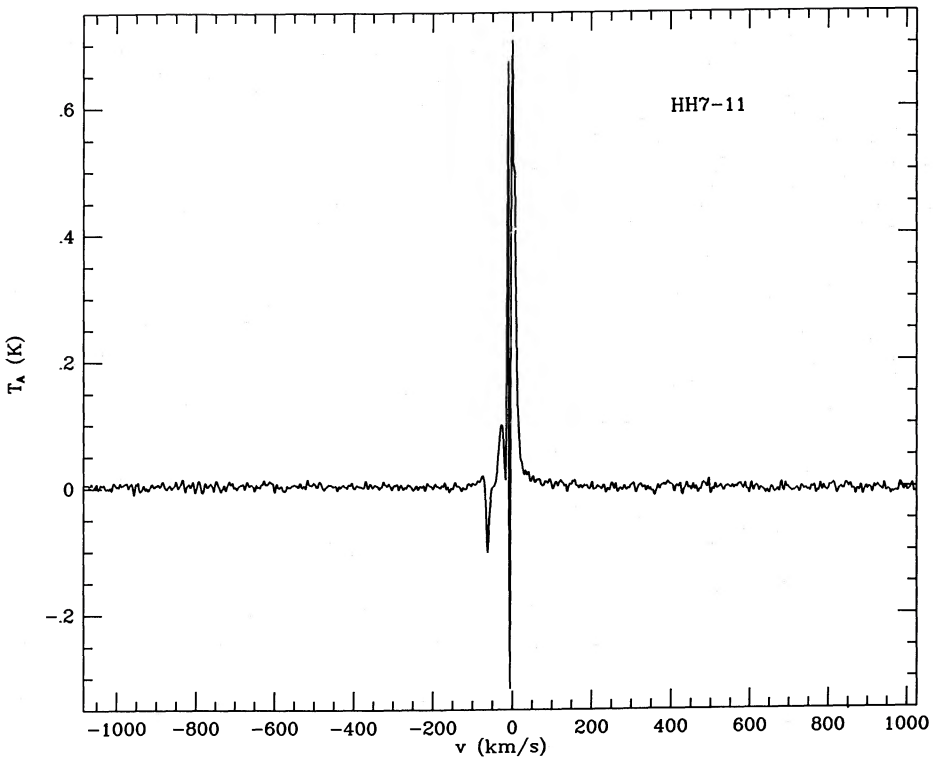

FIG. 1*a*

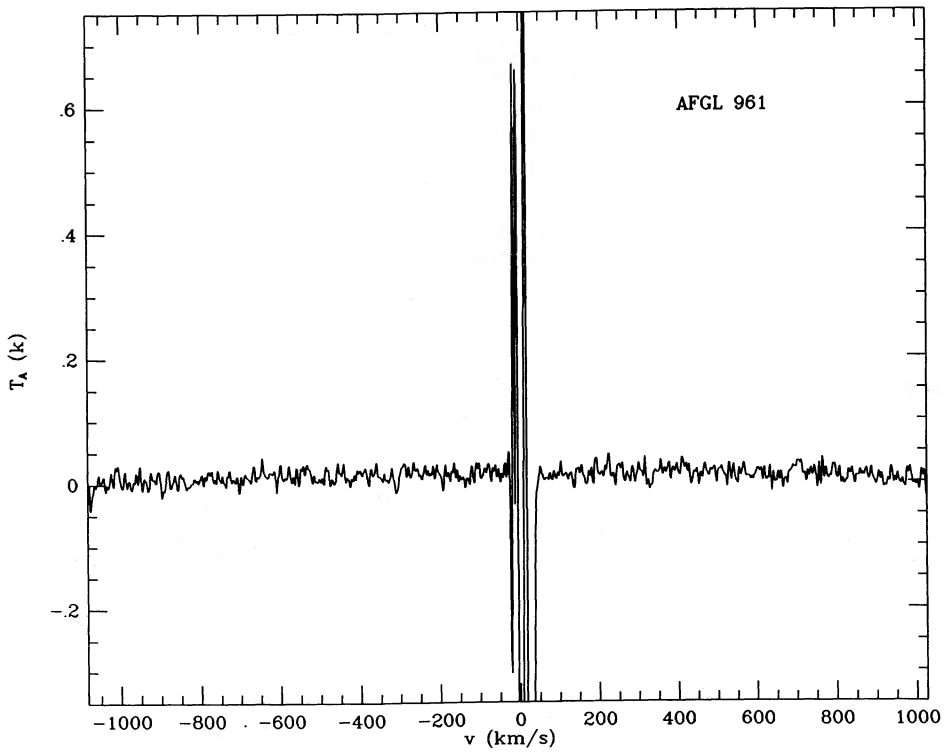

FIG. 1*b*

—H I spectrum taken at Arecibo of (*a*) HH 7–11, and (*b*) AFGL 961. A neutral stellar wind was detected in HH 7–11 and not in AFGL 961.

FIG. 1.

Deep Hα images by Mundt (1984) show that HH 7–11 are the brightest portions of a narrow jet extending away from the position of HH 11 toward HH 7. For HH 11, Herbig and Jones (1983) measure proper motions ~ 60 km s^{-1} pointing away from the SVS 13, which seems to be a deeply embedded object with a bolometric luminosity of $\sim 100\ L_\odot$ (Cohen and Schwartz 1987). The infrared spectral energy distribution of the system has been successfully modeled as a protostar by F. C. Adams (1987, private communication; see Adams and Shu 1986 for the method). The data therefore all indicate that a well-collimated flow is emanating from a central YSO.

a) Mass and Momentum Contained in the Atomic Wind

Figure 1*a* shows the averaged values of five on-source minus off-source spectra at 21 cm for HH 7–11 (with different off positions). The baseline is very flat and one can see excess antenna temperature around the line center up to ~ 97 channels on each side, corresponding to a maximum (wind) velocity along the line of sight of ~ 170 km s^{-1}. Since winds generally reach terminal velocities characteristic of the gravitational well depth from which they escaped, a 170 km s^{-1} wind presumably must originate either directly from the surface of the protostar, or very close to it. The H I emission can be assumed to be optically thin, allowing us to calculate the mass and (absolute value) of the line-of-sight momentum contained in H I from the formulae

$$M_{\rm H} = C \int T_A(v) dv \ , \tag{1a}$$

$$P_{\rm H} = C \int |v|\, T_A(v) dv \ , \tag{1b}$$

where $T_A(v)$ is the antenna temperature at radial velocity v, corrected for the systemic velocity of the molecular cloud. By calibrations on a true point source, the coefficient C in equations (1a) and (1b) can be determined to be

$$C = 3.5 \times 10^{-3}\ {\rm K}^{-1}\ M_\odot\ {\rm km}^{-1}\ {\rm s}\ , \tag{2}$$

if we assume that the distance to HH 7–11 is 350 pc (Herbig and Jones 1983). For an extended source with a uniform brightness temperature over the beam (FWHM = 3.'3), C is a factor $2 \ln (2) \approx 1.4$ larger than equation 2.

Performing conservative integrations by adopting the crude "triangular fit" shown in Figure 2 and assuming that the high-velocity stellar wind in HH 7–11 is unresolved, we obtain from equations (1a) and (1b) the following numerical values for the mass and absolute line-of-sight momentum of the neutral *atomic* wind:

$$M_a = 0.015 M_\odot \ , \tag{3a}$$

$$P_a = 0.87\ M_\odot\ {\rm km\ s}^{-1} \ , \tag{3b}$$

where we have assumed that a cosmic abundance of helium atoms accompanies the H I flow. There is some evidence that the stellar wind may be decelerating by *continuously* transferring its momentum to the ambient molecular gas (see next subsection). In this case, the actual atomic mass and momentum lost from the star integrated for the entire flow history could be significantly larger than the values in equations (3a) and (3b).

A *dynamical* estimate of the integrated mass lost by the star can be obtained as follows. The mass and (absolute line-of-sight) momentum of the molecular flow associated with the CO lobes are, respectively, 2.0 $M_\odot$ and 11 $M_\odot$ km s^{-1} according to

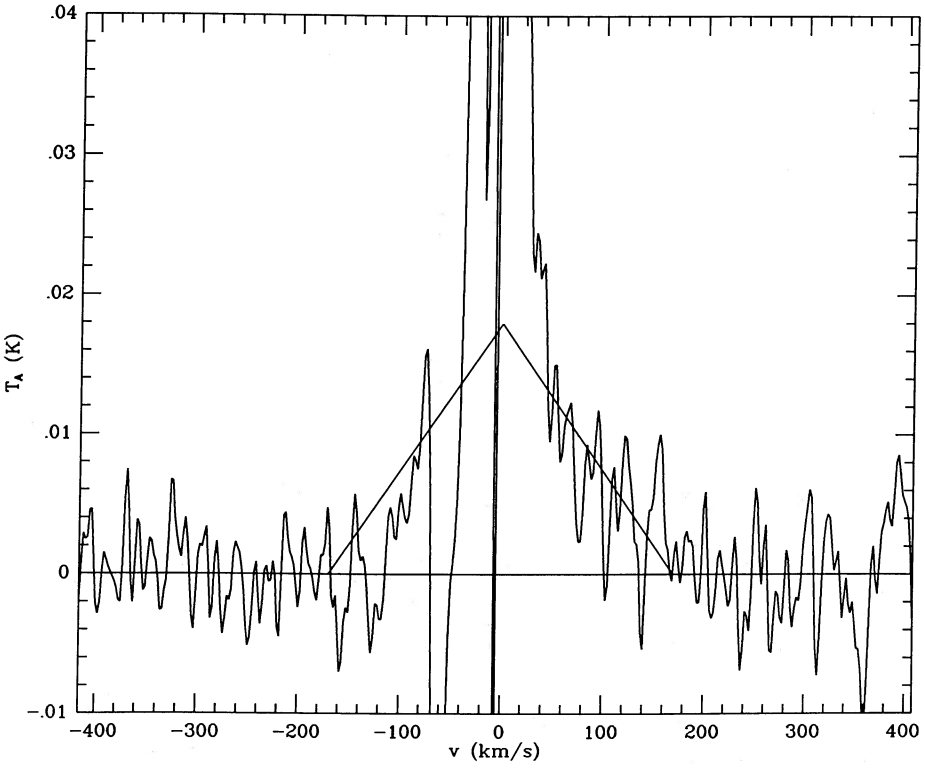

FIG. 2.—Extended line wings in H I of HH 7–11. The atomic hydrogen mass associated with the high-velocity ourflow is taken to be proportional to the area under the triangle. The atomic mass amounts to 0.015 $M_\odot$ (when corrected for a cosmic abundance of helium)..

Edwards and Snell (1984). Let us assume that hydrogen atoms were originally ejected from the star in two beams at 170 km s^{-1} along or away from the line of sight. If the absolute line-of-sight momentum currently observed in the CO lobes came from this atomic stellar wind, then integrated over the entire history of mass loss, the protostar must have lost $\Delta M_* = 11\ M_\odot$ km s^{-1}/170 km $s^{-1} \approx 0.06\ M_\odot$. This is a large total loss of material, but one which is roughly consistent with the interpretation of the line core (see Fig 1) as the total atomic hydrogen accumulated over the lifetime of the flow. As the referee of this paper has pointed out, the structure observed in the core of the line suggests that H I emission exists all around the source and varies significantly on size scales on the order of 10′. Nevertheless, we believe the signal in the line core has significance because if we compute the excess atomic mass in $M_\odot$ at velocities between -50 and $+50$ km s^{-1} for the five independent difference spectra, we obtain -0.06 (north), 0.35 (south), 0.25 (east), 0.21 (west), and 0.25 (bipolar axis). In this calculation we have assumed that the low-velocity material is associated with the source and fills the Arecibo beam. Except for the north offset position, and unlike the case of AFGL 961, the mass excess is systematically positive and close to the value of 0.2 $M_\odot$ for the line core of the average spectrum (see Fig. 1*a*).[4]

If this large loss of protostellar material was accompanied by magnetic braking (cf. Lago and Penston 1982; Lago 1984), then we are in a good position to understand why the optically revealed *pre–main-sequence* counterparts to such objects (of low stellar masses), have such low rates of observed stellar rotation (Vogel and Kuhi 1981; Bouvier *et al.* 1986; Hartmann *et al.* 1986). Indeed, proposals that invoke rapid *protostellar* rotation as the fundamental energy source that powers bipolar outflows now gain additional credence (see, e.g., Draine 1983; Shu and Terebey 1984).

The picture therefore emerges of a stellar wind that continuously decelerates as it entrains material from the ambient medium (see Fig. 3). The line wings represent rapidly flowing atomic material that has an average velocity (for a triangular profile) of 170 km $s^{-1}/3 \approx 60$ km s^{-1}. (We can ignore the deprojection factor for the velocity because the observer lies within the cone of the bipolar flow.) Half of the separation, projected on the plane of the sky, between the centers of the two CO lobes is about 0.12 pc; if we take the bipolar axis to be inclined at an angle $\theta_0 \approx 22°$ (Herbig and Jones 1983), then the deprojected distance from the end of a lobe to the source SVS 13 is 0.12 pc/sin $(\theta_0) \approx 0.3$ pc. The crossing time t_a of the fast atomic hydrogen seen at Arecibo is therefore 0.3 pc/60 km $s^{-1} \approx 5000$ yr. This implies a stellar mass-loss rate $\dot{M}_a = M_a/t_a$ of about $3 \times 10^{-6}\ M_\odot\ yr^{-1}$. If we take the accumulated atomic mass to be $\Delta M_* = 0.2\ M_\odot$, we obtain a flow lifetime $\Delta t = \Delta M_*/\dot{M}_a = 7 \times 10^4$ yr, which is a little longer than the crossing time $R/V_{\rm mean}$ for the extended CO lobes calculated from Table 2 of Edwards and Snell (1984). In other words, two separate arguments indicate that the detected atomic hydrogen wind has sufficient power to drive the observed CO bipolar outflow in HH 7–11.

[4] The total mass lost by the star is difficult to estimate because the demarcation between "line core" and "line wing" is somewhat arbitrary. Our estimate of 0.2 $M_\odot$ for the excess hydrogen in the line core takes into account the suppression of the antenna temperature in the difference spectra by the factor of ~ 2 discussed earlier. It does not include the possibility that, once slowed down, the atomic gas may recombine to molecular form on entrained grain surfaces (Hollenbach, Werner, and Salpeter 1971); simple estimates indicate that the rates associated with this process are only of marginal importance in the present context.

b) Implications of the H I *Line Profile*

It is easy to show that an angularly unresolved, optically thin, spherical wind, moving at a constant terminal velocity, should exhibit a rectangular line profile (for a general discussion, see Bertout and Magnan 1987). (We ignore the broadening and smearing of microturbulence for lines as wide as ± 170 km s^{-1}.) The extreme velocities would equal the terminal velocity (after subtraction of the velocity of the molecular cloud to take out the likely motion of the central protostar), and the area under the curve will be proportional to the total mass of atomic hydrogen. If the wind blows only in two oppositely directed cones of opening angle α centered about the z-axis, which makes an angle θ_0 to the line of sight of the observer (see Fig. 3), the line profile will still be flat-topped if the other conditions hold, but there may be missing portions of the previously available range of velocities, depending on the exact values of α and θ_0. This occurs for the following simple reason. Consider a given element of hydrogen gas at spherical polar coordinates (r, θ, ϕ) relative to the protostar (with the observer placed in the x-z plane), and suppose this gas moves outward at a radial speed $v_{\rm H}$ relative to the protostar. It then has the line-of-sight velocity v relative to the observer given by

$$v = v_{\rm H}(\cos\theta_0 \cos\theta + \sin\theta_0 \sin\theta \cos\phi)\ . \qquad (4)$$

For ejection in a cone, ϕ has unrestricted range (from 0 to 2π), but θ is confined to lie between 0 and $+\alpha$ (for the upper cone). The maximum value of $|v|$ is then $v_{\rm H} \cos(\theta_0 - \alpha)$ if $\theta_0 > \alpha$ and $v_{\rm H}$ if $\theta_0 < \alpha$; the minimum value, either $v_{\rm H} \cos(\theta_0 + \alpha)$ or 0, whichever is larger.

But Figure 2 shows that the 21 cm line profile does not have a flat-topped shape, neither a whole rectangle appropriate for a spherical constant-velocity wind, nor a sum of rectangles, appropriate for a biconical constant-velocity wind observed nearly pole-on. Instead, the line profiles have continuously declining wings of high-velocity gas, implying that there is more atomic hydrogen at low velocities compared to high velocities than should have been present in the constant wind-velocity models. The sloping wings cannot be reproduced by a constant wind-velocity model where the atomic hydrogen steadily recombines into molecular hydrogen as the flow proceeds, because each spherical shell of material would still produce a rectangular line profile, and the sum of all such constant velocity shells would be rectangular. Moreover, once the wind reaches any appreciable distance from the central protostar, the densities become too low for all recombination processes other than on grain surfaces, and it is unlikely that grains would exist in an outflow from a star at the likely effective temperature $\sim$6000–7000 K of SVS 13 (F. C. Adams 1987, private communication).

Entrainment of ambient molecular gas might introduce interstellar grains into the flow, but the more important effect in that case is a *mechanical deceleration* of the wind as it propagates. This deceleration will generally produce a resultant velocity field in the original hydrogen gas that (apart from a fluctuating turbulent component) depends on both radial distance r and angular position θ from the ejection axis, $v_{\rm H} = v_{\rm H}(r, \theta)$. For kinematic modeling purposes, it is convenient to suppose that the r and θ dependences separate,

$$v_{\rm H}(r, \theta) = V(r)\Theta(\theta)\ . \qquad (5)$$

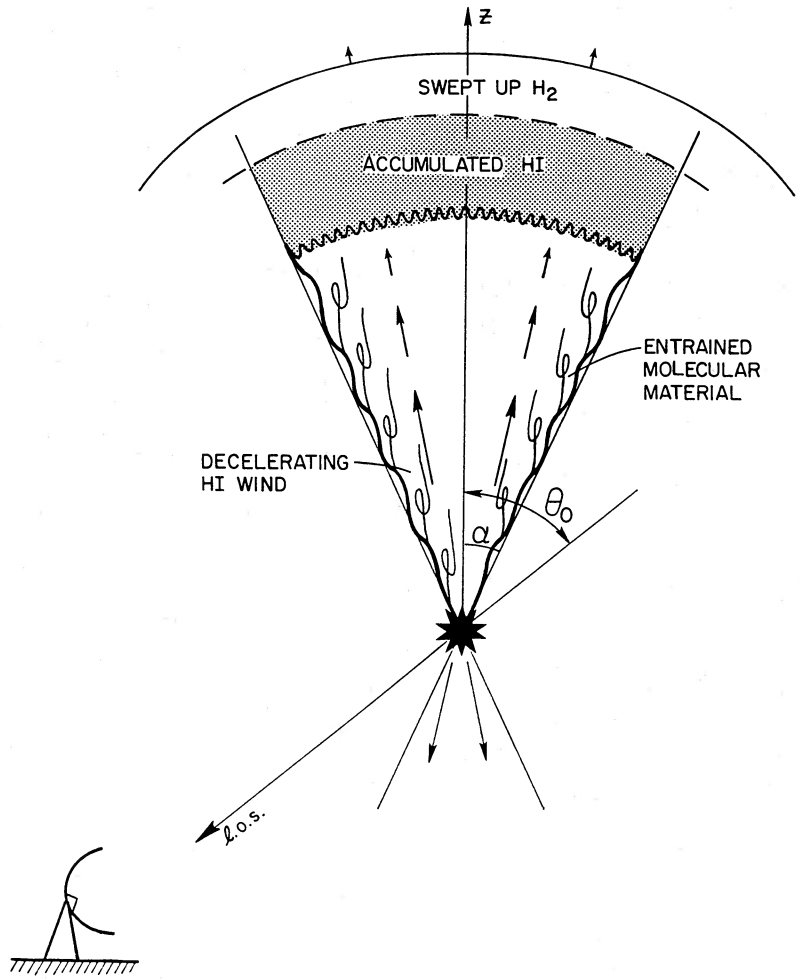

FIG. 3.—Schematic picture of the entrainment process for one cone of a bipolar outflow. Close to the central protostar, the stellar wind has a high (terminal) velocity. Farther out, entrainment of molecular gas occurs through instabilities on the interface between the wind flow and the ambient cloud core. The incorporation of additional mass into the outflow steadily decelerates the original atomic wind, accounting for the non rectangular nature of the H I line profile in Fig. 1. The outflow material encounters a shock (*wavy curve*) at the end of its trajectory, and accumulates in a shell of relatively slowly moving gas that is observed as the core of the H I line profile in Fig. 1. The outwardly plowing shell of accumulated stellar wind (plus entrained matter) drives another shock (*solid curve at the top of the figure*) into the ambient cloud, behind which follows the swept-up H_2 gas observed as the classical CO lobes in bipolar flows. In accordance with the standard picture of wind-driven bubbles, the swept-up molecular gas and the accumulated stellar outflow, which move outward at almost the same speed if the shocks are strongly radiative, are separated by a contact discontinuity (*dashed curve*).

In an examination of the line profiles of forbidden-line emission from YSO outflow sources, Edwards *et al.* (1987) obtained reasonable fits by choosing V = constant and various trial forms for Θ. Their interpretation did not invoke entrainment but attributed the variations in the flow field as being intrinsic to an *anisotropic* ejection mechanism close to the surface of the star. This interpretation may well have merit, but our HCO^+ measurements to be discussed in the next subsection suggest that entrainment is also present (at larger distances than considered by Edwards *et al.*); consequently, we investigate, as an extreme alternate possibility, the complementary case Θ = constant = 1.

In particular, for an optically thin biconical outflow, the Appendix shows that a power-law velocity of the form $V(r) = Ar^{-1/\beta}$ will produce a power-law line profile:

$$T_A(v) = \frac{\dot{M}_H A^\beta}{C|v|^{2+\beta}} f(\theta_0, \alpha, \beta) , \qquad (6)$$

where $\dot{M}_H$ is the hydrogen mass-loss rate in *one* cone and $f(\theta_0, \alpha, \beta)$ is a dimensionless form function that has a known dependence on the observing angle θ_0, opening angle α, and deceleration exponent β. (See eqs. [A8] and [A9] for important examples. If HH objects arise from a shocked neutral wind, the observations of Cohen and Jones [1987] favor $\beta = 1$.) Since our H I observations are angularly unresolved, we cannot use them to obtain the geometrical parameters α and θ_0 that enter in the expression for f. The ratios of tangential to radial velocities of the HH objects suggest that $\theta_0 \approx 22°$ (Herbig and Jones 1983). The (averaged) ratio of CO lobe sizes to the (deprojected) displacement from SVS 13 (see Snell and Edwards 1981) suggests $\alpha \approx 30°$. With $\beta = 1$, equation (A8) then implies that $f = 0.8$. With $\beta = 2$, equation (A9) gives $f = 1.3$.

The inverse power-law in r for the flow velocity $V(r)$ cannot hold, of course, for arbitrarily small or large values of r; consequently, in actual application, equation (6) should not be considered valid in the limits $|v| \to 0$ (where the residual wind may be arrested in a final shock by slamming head-on into the

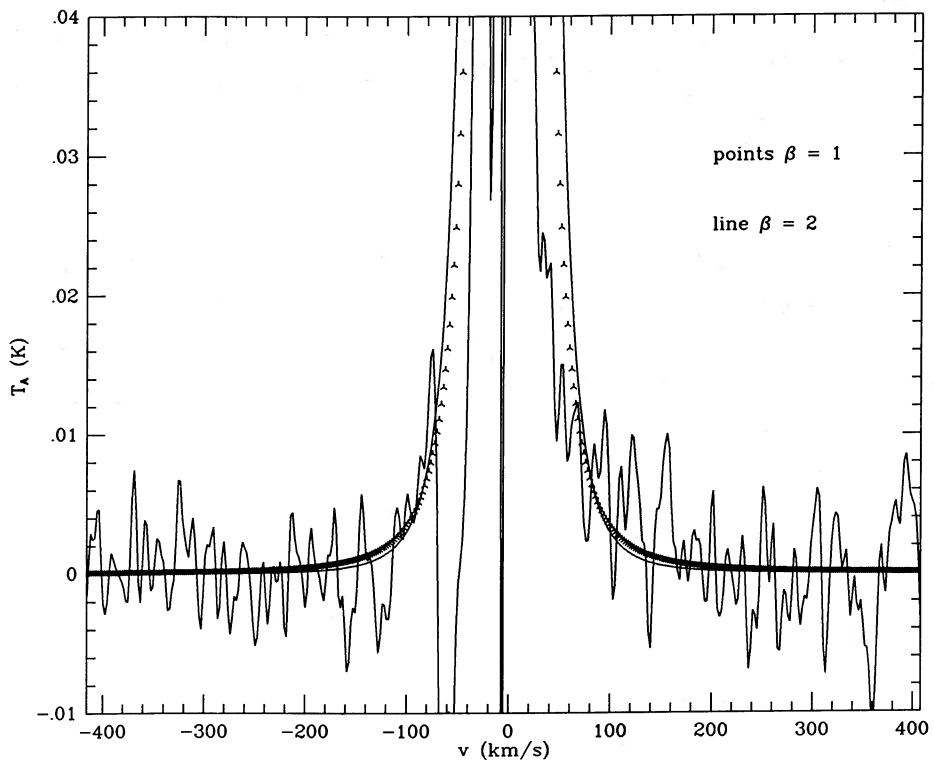

FIG. 4.—Power-law fits to the extended line wings of HH 7–11 of the form $T_A = B|v|^{-(2+\beta)}$ (see eq. [6])

ambient medium), or when $|v|$ exceeds some reasonable terminal velocity along the line of sight. As Figure 4 demonstrates, however, the power-law $T_A(v) = B|v|^{-(2+\beta)}$, with β between 1 and 2, fits the data acceptably well over the intermediate velocity interval, where we expect to find the decelerating wind in accordance to Figure 3. For $\beta = 1$, we obtain $B = 3.5 \times 10^3$ K km^3 s^{-3}. For $\beta = 2$, we obtain $B = 3.0 \times 10^5$ K km^4 s^{-4}. In either case, the tendency of the low-velocity data to fall below the theoretical spectra is not particularly alarming given the reasons expounded upon in the previous subsection concerning why the line core may be undermeasured by the experiment.

From the formal fit for the constant

$$B = \dot{M}_H A^\beta f / C , \qquad (7)$$

we may estimate the deceleration coefficient A and compare the derived value with various observational constraints. For a hydrogen mass-loss rate in *one* cone, $\dot{M}_H = X_H \dot{M}_a/2$, where $X_H = 0.7$ is the hydrogen mass abundance and $\dot{M}_a = 3 \times 10^{-6}$ $M_\odot$ yr^{-1} is the atomic mass-loss rate in *both* cones, we obtain $A = 15$ km s^{-1} pc for $\beta = 1$, and $A = 27$ km s^{-1} pc$^{1/2}$ for $\beta = 2$. With such values, the wind velocity $V(r) = Ar^{-1/\beta}$ equals 50 km s^{-1} at $r = 0.3$ pc for $\beta = 1$ or 2. The wind has its terminal velocity 170 km s^{-1} at $r = 0.09$ pc for $\beta = 1$, and at $r = 0.025$ pc for $\beta = 2$. Outside of this fiducial radius, the interaction with the ambient medium would begin to decelerate the stellar wind; inside, it would presumably maintain a constant velocity if we are to have a reasonable physical picture.

The HCO^+ observations to be discussed in the next subsection support our interpretation that wind deceleration and entrainment of ambient material is occurring in the bipolar flow of HH 7–11. In particular, the deceleration lengths deduced in the above model are consistent with the detection of enhanced HCO^+ emission, on angular scales of the Nobeyama and Kitt Peak radio telescopes, at velocities intermediate between the Arecibo H I and the extended CO lobes. Finally, our model of continuous entrainment implies that the wind material will shock and will be brought to a velocity comparable to that of the extended CO lobes ($\sim$27 km s^{-1}), at only a fraction of the full "terminal" speed of the stellar outflow.

c) *Molecular Line Observations*

We next observed HH 7–11 with the 45 m radiotelescope in Nobeyama, Japan, in ^{12}CO, in HCO^+, and in HCN (all $J = 1$–0) at angular resolutions of 16″, 20″, and 21″ respectively. The observations were made by position switching once per minute 5′ to the north of the source for a total observing time of 50 minutes. The top two panels of Figure 5 (different spectrometers measuring the $J = 1$–0 line) show that the CO profile has velocity wings that reach at least to $\pm$50 km s^{-1}, and perhaps to -100 km s^{-1} in the blueshifted wing (but with poor signal-to-noise ratio). Such velocities are well beyond the known velocity range $\pm$27 km s^{-1} of the *extended* CO emission on the arcminute scales of the bipolar lobes (Edwards and Snell 1984). The third panel of Figure 5 of the HCO^+ emission gives more secure evidence that molecular material is present at higher velocities than those conventionally associated with the bipolar outflow. In HCO^+ one sees a strong blueshifted wing, with a weaker counterpart on the redshifted side. On the blueshifted side, there is emission that extends to -100 km s^{-1}, intermediate to the highest velocities seen in H I and extended CO. We believe the HCO^+ emission to arise from ambient molecular gas that has been entrained in the H I stellar wind en route to sweeping up the more extended classical lobes of CO emission. This entrainment then ultimately leads to the deduced deceleration that was discussed in the

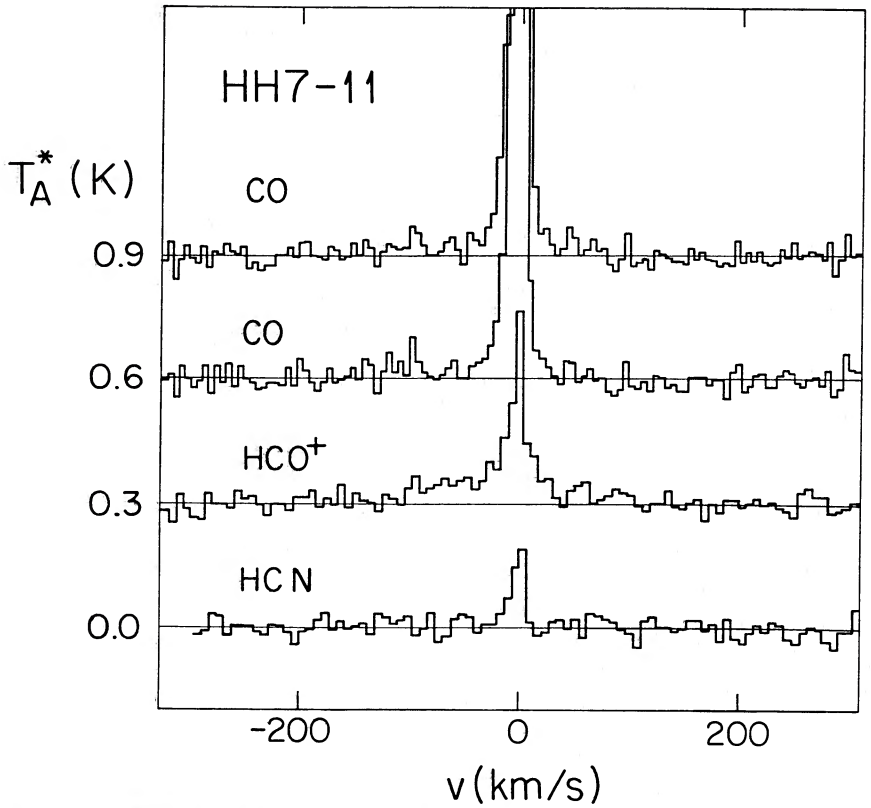

FIG. 5.—CO, HCO^+, and HCN spectra of HH 7–11 taken at Nobeyama. The top two panels for CO show the measurements of two different spectrometers; marginal indications exist for high-velocity gas, but the spectrum is quite noisy. The HCO^+ spectrum shows evidence for (entrained) material (of enhanced HCO^+ abundance) up to ± 70 km s^{-1}; the HCN spectrum shows only low-velocity gas (of normal molecular abundance).

previous subsection. Our failure to detect an equally strong red wing in HCO^+ suggests a somewhat unequal interaction of the outflowing H I wind with the ambient material at the $\pm 10''$ scale on the two sides of the protostar.

If we assume that the HCO^+ is optically thin and that the ambient densities are high enough to thermalize the population of lower rotational levels at a kinetic temperature T, we may derive the mass and absolute line-of-sight momentum contained in HCO^+ in a manner analogous to our treatment for H I. The values associated with the *blueshifted wing only* are

$$M_{HCO^+} = 8 \times 10^{-9}(T/100\ \mathrm{K})\ M_\odot\ , \quad (8a)$$

$$P_{HCO^+} = 4 \times 10^{-7}(T/100\ \mathrm{K})\ M_\odot\ \mathrm{km\ s^{-1}}\ . \quad (8b)$$

Assuming that the number abundance of HCO^+ relative to H_2 is $3 \times 10^{-9}\eta$, with $\eta = 1$ for normal interstellar values (see, e.g., Vogel *et al.* 1984; Irvine, Goldsmith, and Hjalmarson 1987), we obtain a mass and momentum contained in the entrained *molecular* gas (including helium) equal to

$$M_m = (0.3/\eta)(T/100\ \mathrm{K})\ M_\odot\ , \quad (9a)$$

$$P_m = (13/\eta)(T/100\ \mathrm{K})\ M_\odot\ \mathrm{km\ s^{-1}}\ , \quad (9b)$$

for the blueshifted component.

Depending on whether one relies on the CO measurements of Edwards and Snell (1984) or on the H I deductions of § III*a*, the blueshifted lobe of the CO flow contains a line-of-sight momentum from 5 to 18 $M_\odot$ km s^{-1}. Since the crossing time associated with the HCO^+ is ~ 30 times shorter than the corresponding value for the (more extended and slower) CO bipolar flow, the momentum carried in the molecular gas at a $10''$ radial scale (imparted to it presumably by the atomic stellar wind) is 20–80 times greater than needed to drive the observed CO motions *if* $T = 100$ K and $\eta = 1$. Since T is unlikely to be much smaller than 100 K, this suggests that η is actually $\gg 1$.

The dynamical argument given above that the anomalous abundance of HCO^+ arises from interaction of a stellar outflow with the ambient molecular cloud gains support from the interferometric study at the Hat Creek Radio Observatory by Rudolph and Welch (1988) who found stationary HCO^+ emission to lie *ahead* of HH 9, 10, and 11. It is also supported by our Nobeyama result that the high-velocity wings appear (if at all) with lower strength in CO than in HCO^+. Independent of any assumption concerning T (except that it be high enough to thermally populate the lower rotational levels of both molecules), the $J = 1$–0 line of CO *should have been stronger* by a factor of ~ 40 than the corresponding transition in HCO^+ *if their number abundances were normal* (5×10^{-5} and 3×10^{-9} relative to H_2). Since the signal in the CO high-velocity wings is smaller than in the HCO^+ wings for simultaneous observations with similar beamsizes, HCO^+ must be enhanced by a factor $\eta > 40$ in the regions under consideration. The larger enhancement is apparently peculiar to this molecular ion since HCN (Fig. 5, fourth panel) does not show anomalous emission strength. In this regard we mention that a tenfold HCO^+ enhancement has been found in the shocked molecular gas associated with the supernova remnant IC 443 (DeNoyer and Frerking 1981).

The conclusion arrived at above was verified by higher signal-to-noise ratio observations carried out on the 12 m dish

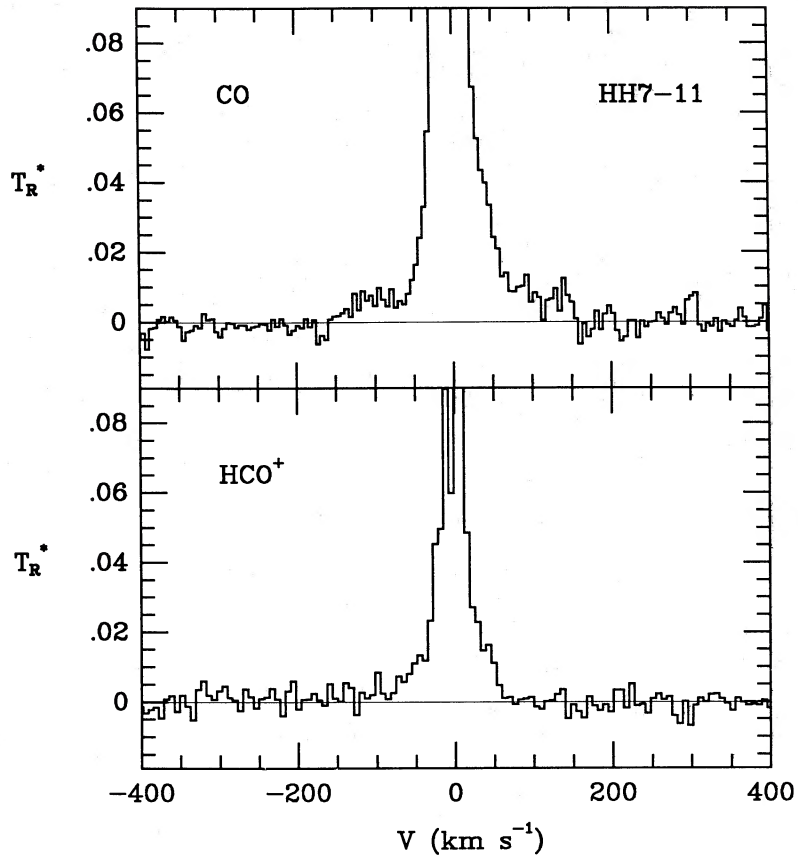

FIG. 6.—Spectra of HH 7–11 taken at Kitt Peak in (*top*) CO and (*bottom*) HCO^+. The line wings in CO extend to $\sim \pm 160$ km s^{-1} and can be interpreted in terms of a direct observation of the outflowing stellar wind before much interaction has occurred with the ambient molecular gas. As true also for the Nobeyama spectrum, the HCO^+ reach only ± 70 km s^{-1}, indicating that this material consists of entrained molecular gas. The similar CO and HCO^+ line intensities at intermediate velocities in the line wings demonstrate that the HCO^+ abundance has been considerably enhanced by the interaction of the stellar wind with the ambient molecular cloud. (Notice that the radiation temperature plotted here T_R^* is related to the antenna temperature via $T_R^* = T_A^*/\eta_{fss}$, where the forward spillover and scattering efficiency for the Kitt Peak 12 m telescope is $\eta_{fss} = 0.75$ [Kutner and Ulich 1981]).

at Kitt Peak (see Fig. 6). The angular resolution is 1′ for CO and 1.′2 for HCO^+. The experiment was performed by beam switching with the tiltable subreflector once per second in azimuth to a displacement of 4′ and 6′ in both directions from the central source. The total observing time spent on HH 7–11 was 12 hr in CO and 2 hr in HCO^+. Except for a slight overall displacement to positive velocities, the line profiles are now almost symmetrical and show extensions that reach to ± 160 km s^{-1} for CO and ± 80 km s^{-1} for HCO^+. On radial scales of $\sim 30''$, the blueshifted and redshifted gas evidently does not exhibit large asymmetries. In the sloping line wings at intermediate velocities (say, ± 50 km s^{-1}), the CO to HCO^+ intensities again show an anomalous ratio ($\sim 1:1$). This yields a strong indication that the interaction suffered by entrained molecular gas at intermediate velocities can cause the HCO^+ abundance to become significantly enhanced over normal interstellar values. A more normal (and much higher) CO to HCO^+ ratio applies to the line core, but the signal at low velocities could be contaminated by emission or absorption in the surrounding molecular gas.

Within the signal-to-noise ratio, the line profiles obtained at Nobeyama and Kitt Peak appear consistent with one another, especially if we take into account that the different beam sizes of the two telescopes may sample different amounts of the decelerating wind flow and entrained molecular gas (see Fig. 3). This comment applies with even greater force to the apparent differences between the H I and CO line shapes.

Unlike the H I seen in Figure 1, the CO line profile of Figure 6 (*top*) gives a clear indication for *two* separate components: (1) a central line-core of low-velocity gas which *smoothly* blends into a declining wing of intermediate-velocity gas, and (2) a roughly *rectangular* component that extends to ± 160 km s^{-1}. The first feature suggests a *continuous* process of entrainment of ambient molecular gas and deceleration of the outflow to the classical CO lobe velocities; the second, a direct view of the neutral stellar wind before much interaction with the surrounding material has taken place. Presumably, a shallow and broad rectangular profile at high velocities was not clearly observed at Arecibo because of insufficient angular resolution and at Nobeyama because of insufficient signal-to-noise ratio.

To analyze the implications of the high-velocity CO observations, we assume that the stellar winds seen directly in CO and H I occupy the same spatial location, and that the flows (in accordance with the model of § III*b*) are angularly unresolved at both Kitt Peak and Arecibo. The number abundance of CO relative to H I is then given by the ratio of column densities associated with the relevant (high) velocity interval:

$$\frac{N_{CO}}{N_{HI}} = 1.5 \times 10^{-4}\left(\frac{T}{100\ \mathrm{K}}\right)\frac{\int T_A^{CO}\,dv}{\int T_A^{HI}\,dv}, \qquad (10)$$

where we have incorporated a factor of 15 to account for the difference in telescope response to point sources at Kitt Peak and Arecibo. If we ignore the difference in line shapes of the Kitt Peak and Arecibo data and if we assume that the kinetic temperature T is or order 10^2 K (observations of CO at higher J-transitions would help to pin down T), the ratio of line intensities of CO and H I at high velocities in Figures 2 and 6 (*top*) (say, between 70 and 150 km s^{-1}) implies that the number abundance of CO relative to H I is consistent with most of the carbon being in the form of CO. (The cosmic number abundance of C relative to H is 4×10^{-4}.) Conversely, if we assume that a wind originates from the surface of a protostar where the hydrogen is atomic and all of available carbon is in the form of CO (or soon acquires this state as the gas expands and cools), then the two experiments measured identically the same flow.

IV. RESULTS FOR L1551 IRS 5

Of the other sources we observed at Arecibo (see Table 1), only L1551 IRS 5 showed any evidence of high-velocity atomic gas. Unfortunately, the evidence is unambiguous only in one of three difference spectra, when the off-source position was 10′ *west* of the protostar. For off-source positions of 10′ *east* and *north* of the protostar, the difference spectra are badly chopped up by many narrow features due probably to small clouds along the line of sight. Even for the one positive detection, a high-velocity wing is apparent only on the redshifted side of the line (see Fig. 7); the blueshifted side shows similar chopped-up features as obtained with the east and north reference positions. (The result is an exaggerated version of what also happens in HH 7–11, but in L1551, because we are looking at the system nearly equator-on, we do not have the benefit of wings of very high-velocity gas.) The simplest interpretation of this phenomenon is that (blueshifted) high-velocity H I clouds are known to exist in the part of the sky toward L1551 (a suspicion confirmed by measurements using the Hat Creek 85 foot [26 m] dish), and that small-scale structures in these clouds (as well as in clouds of lower velocity) contaminate the blueshifted component of the high-velocity stellar wind, making its identification quite uncertain (see also Mirabel, Cantó, and Rodríguez 1983). In principle, the narrowness of the spurious spectral features would allow their rejection, but the integration time (75 minutes) spent on L1551 was 3 times less than HH 7–11 (where the high-velocity wings and positive central spike were seen relative to all five reference positions). A dedicated mapping program in H I at high signal-to-noise ratio may provide a solution of this difficulty. Until then, we shall analyze only the case when the west reference position was used.

Since L1551 IRS 5 is at a distance of 140 pc (Elias 1978) and since the Arecibo beam is ~ 8 times smaller than the known extent of the CO lobes, we shall assume that the stellar outflow is (partially) resolved by the beam. If we adopt the assumption of a uniform source brightness temperature in the beam, the coefficient C in equations (1a) and (1b) for L1551 IRS 5 is given by

$$C = 7.8 \times 10^{-4}\ \mathrm{K}^{-1}\ M_\odot\ \mathrm{km}^{-1}\ \mathrm{s}\ . \tag{11}$$

The atomic mass and line-of-sight momentum associated with the triangular representation of the wings of the H I line in Figure 7 are

$$M_a = 6 \times 10^{-3}\ M_\odot\ , \tag{12a}$$

$$P_a = 0.1\ M_\odot\ \mathrm{km\ s}^{-1}\ . \tag{12b}$$

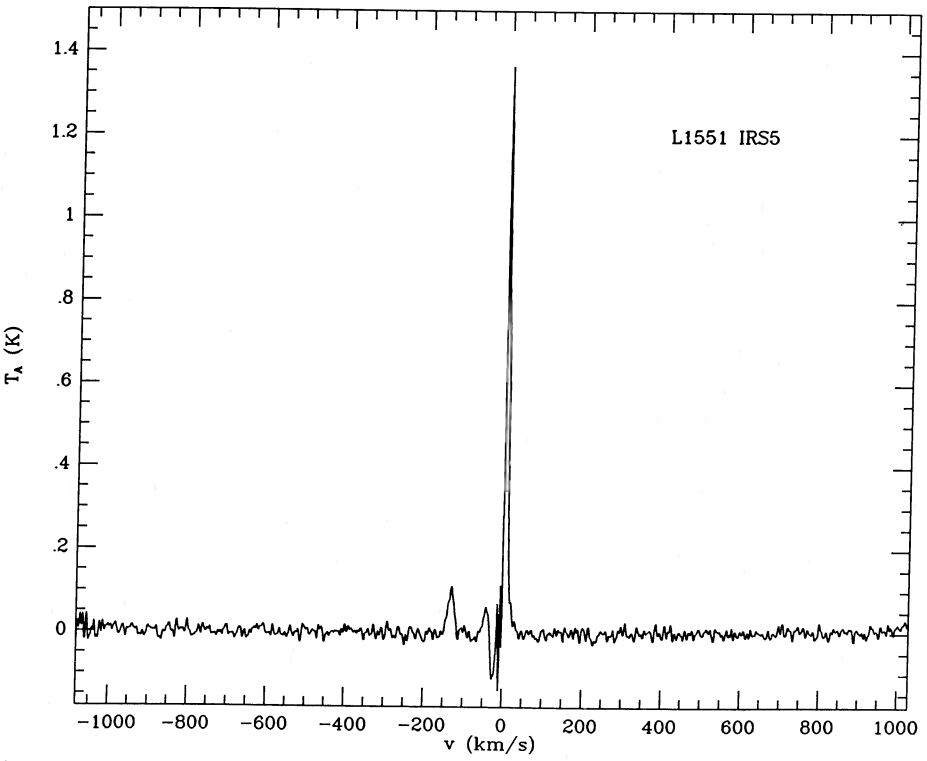

FIG. 7.—H I spectrum taken at Arecibo of L1551 IRS 5 referenced with respect to an off-position 10′ west of the source. Since this source is being viewed nearly equator-on, the evidence for a neutral stellar wind is less cogent than for HH 7–11 because of contamination by high-velocity Galactic H I gas.

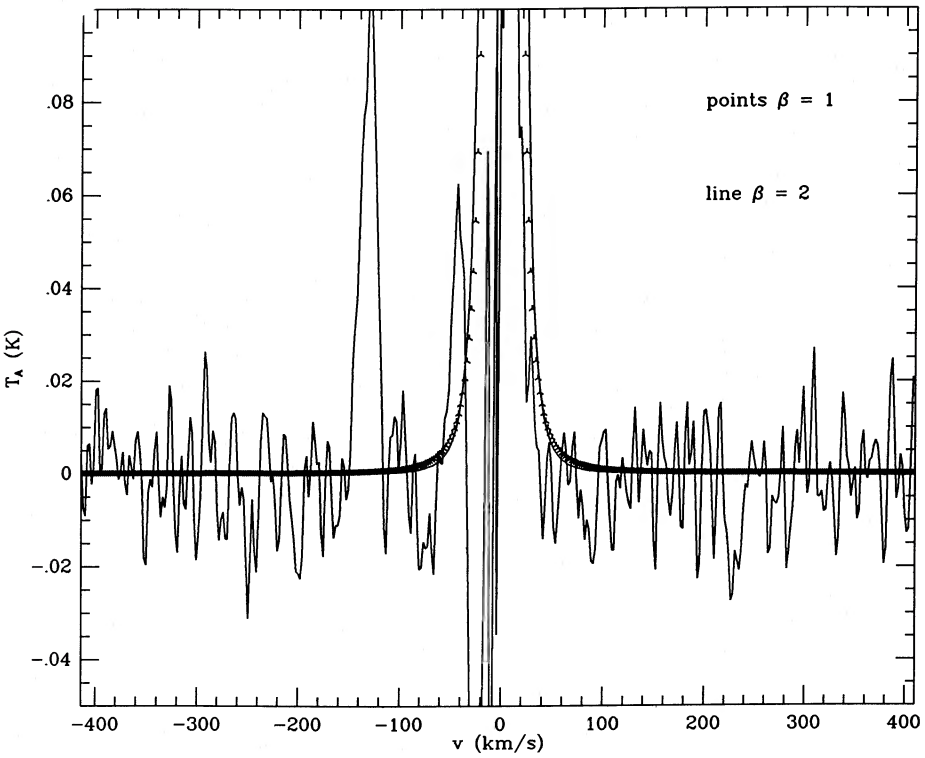

FIG. 8.—Power-law fits to the extended line wings of L1551 IRS 5 of the form $T_A = B|v|^{-(2+\beta)}$ (see eq. [6])

Because the observed H I velocities are ~3–4 times greater than those of the CO lobes, while the Arecibo beam is ~8 times smaller than the extent of the CO lobes, the crossing time associated with the H I must be ~30 times smaller than the corresponding value for the CO. If we take the latter to be 4×10^4 yr (Snell and Schloerb 1985), then the implied mass-loss rate is $4 \times 10^{-6}\ M_\odot\ \mathrm{yr}^{-1}$. (In L1551 we are unable to use the accumulated atomic hydrogen to independently estimate the total flow time because the Arecibo beam is too small to cover an appreciable fraction of the outermost flow.)

Let us now briefly analyze the line shape (see Fig. 8). The redshifted wing of the atomic gas extends out only to $\sim +50$ km s^{-1} because L1551 IRS 5 has a well-collimated flow seen nearly edge-on. The ratio of radial to tangential velocities of the associated HH objects (Strom, Grasdalen, and Strom 1974; Cudworth and Herbig 1979) implies that $\theta_0 \approx 75°$ (Snell and Schloerb 1985). The terminal velocity V_* of the wind is then ~ 50 km s^{-1}/cos $(\theta_0) \approx 190$ km s^{-1}. The CO map of the bipolar flow (Snell, Loren, and Plambeck 1980) suggests that $\alpha \approx 10°$–$20°$. Equations (A8) and (A9) yield $f \approx 0.07$, relatively insensitive to the precise choice of α and whether we use $\beta = 1$ or 2. For $\beta = 1$, a line profile fit yields $B = 9.6 \times 10^2$ K km^3 s^{-3}; for $\beta = 2$, $B = 3.8 \times 10^4$ K km^4 s^{-4}. The corresponding deceleration coefficients A are 7.8 km s^{-1} pc and 18 km s^{-1} pc$^{1/2}$. The implied entrainment rates are qualitatively consistent with measurements of OH seen in absorption against the cosmic microwave background. From such observations, Mirabel *et al.* (1985; see also Clark and Turner 1987) found molecular gas moving at intermediate velocities on radial scales $r \approx 0.2$ pc.

Using the mass-loss rate, $\dot{M}_a \approx 4 \times 10^{-6}\ M_\odot$, we calculate that a stellar wind with a line-of-sight terminal velocity of 50 km s^{-1}, and lasting for $\sim 4 \times 10^4$ yr, can approximately provide the total line-of-sight momentum associated with the CO bipolar flow of this source, 5.3 $M_\odot$ km s^{-1} (see Snell and Schloerb 1985). Thus, the observed atomic wind satisfies the *integrated* momentum requirement. The mechanical luminosity inferred to be *currently* in the wind is $\dot{M}_a V^2/2 \approx 12\ L_\odot$, one-fourth of which will be deposited at large radii when the wind has decelerated to one-fourth of its original velocity (under momentum conservation by entraining ambient gas to a total of 4 times its original mass). Such a picture would account for the excess far-infrared luminosity deduced by Edwards *et al.* (1986) ($\sim 3\ L_\odot$ beyond the CO lobes). Therefore, the tentatively observed atomic wind also yields the correct *instantaneous* energetic requirement.

V. SUMMARY

For the other cases in Table 1, we detected no obvious high-velocity H I. These objects, which are fairly luminous sources, must also have drivers for their observed CO outflows. C. Bertout (1987, private communication) and Cantó, Dyson, and Rodríguez (1987) believe that the mass and momentum associated with the CO outflows from high-luminosity sources may have been considerably overestimated in previous work, and that no momentum deposition beyond radiatively driven winds is required for such objects. If this suggestion proves to be correct, then the need for neutral stellar winds may be confined to low luminosity bipolar flow sources. For very cool protostars, the neutral stellar wind may become largely *molecular* (H_2) as it leaves the stellar surface. This is known to happen in the case of evolved stars) see, e.g., Glassgold and Huggins 1983), although the fraction of the hydrogen in the wind that is H_2 rather than H I depends sensitively on the precise conditions of gas temperature, density, and (small) ionization fraction near the star. Nevertheless, as the case of HH

7–11 demonstrates, the stellar wind may be atomic as far as H I versus H_2 goes, yet still contain the extremely stable molecule CO.

We summarize below the most important conclusions that we have drawn from the positive results of this paper.

1. In HH 7–11, from direct observations of H I line wings, we deduce that there exists instantaneously an atomic mass $\sim 1.5 \times 10^{-2}\ M_\odot$ associated with rapidly flowing gas. The stellar mass-loss rate is, therefore, $\dot{M}_a \approx 3 \times 10^{-6}\ M_\odot\ \mathrm{yr}^{-1}$ if the crossing time of the (decelerating) wind is 5×10^3 yr.

2. The excess emission (above background) in the H I line core, which we associate with *accumulated* stellar atomic hydrogen, gives a total duration of the outflow $\sim 7 \times 10^4$ yr.

3. A detailed analysis of the H I *line shape* yields a reasonable deceleration rate for the atomic wind if we adopt the view that the stellar wind continuously entrains ambient molecular gas as it propagates from the protostar. Our Nobeyama data indicate that the entrainment process is already well underway at radial scales 10″ from the protostar. The smoothness of the CO and HCO^+ line profiles at low and intermediate velocities obtained at Kitt Peak suggests a picture of gradual deceleration by continuous entrainment, rather than by a single shock jump at the end of the flow (although the latter may also be present). Clearly, resolved interferometric maps of the entire flow region would be very interesting.

4. A stellar wind with a terminal velocity of 170 km s^{-1} and with a mass-loss rate of the magnitude indicated by our 21 cm line observations, lasting $\sim 7 \times 10^4$ yr, would (more than) suffice to drive the known extended CO bipolar outflow in HH 7–11. The same stellar wind has been detected in very high-velocity CO gas, where the line profile beyond ± 70 km s^{-1} does show, within the considerable noise, the rectangular shape that one expects for a constant velocity biconical flow viewed more-or-less pole-on. Notice that unlike the case of the normal interstellar medium, CO coexists with H I in the flow from the atmosphere of this relatively cool protostar.

5. If the HCO^+ gas seen at small angular scales and at intermediate velocities is interpreted as entrained molecular gas, too great a stellar loss of mass and momentum would be implied compared to the above values unless the abundance of HCO^+ has been enhanced by a factor 20–80. A large enhancement of order 40 is directly indicated by our Kitt Peak data of HCO^+ and CO emission at intermediate velocities.

6. In L1551 IRS 5, our H I observations allow us to deduce an atomic mass-loss rate, $M_a \sim 4 \times 10^{-6}\ M_\odot\ \mathrm{yr}^{-1}$. With a deduced terminal velocity $V_* \approx 190$ km s^{-1}, the stellar wind possesses enough integrated momentum to drive the observed CO bipolar flow and enough instantaneous mechanical luminosity to account for the excess extended far-infrared radiation seen in this source.

7. The "detection" of rapidly moving H I gas in L1551 IRS 5 must be regarded as tentative since it is badly contaminated by the presence of Galactic hydrogen at similar velocities in this general direction.

We conclude that stellar winds with low ionization fractions may provide the underlying power of bipolar flows from low-mass protostars. Since the observed winds have velocities comparable to the escape velocities from the surfaces of such stars, they cannot originate from the shallow potential-well depths associated with large circumstellar disks. With respect to ordinary stellar winds, apart from fundamental difficulties with radiative losses at high mass-loss rates (see, e.g., DeCampli 1981), thermally driven coronal winds based on a solar analogy would seem to be eliminated by our results. Much more viable, in our opinion, are mechanisms that invoke momentum deposition in winds driven by Alfvén waves or centrifugally from the surface of a magnetically active and rapidly rotating protostar (Hartmann and MacGregor 1981, 1982).

We thank P. Carral, A. Rudolph, and T. Troland for their help and illuminating suggestions. We also acknowledge informative discussions with F. Adams, G. Basri, C. Bertout, J. Beiging, G. Herbig, R. Plambeck, and W. J. Welch. This work was funded in part by grants from the National Science Foundation; from the NASA astrophysics program which supports a joint Center for Star Formation Studies at UC Berkeley, UC Santa Cruz, and NASA/Ames Research Center; from CONACYT, México; and a fellowship from the National University of Mexico.

APPENDIX

POWER-LAW VELOCITY LAWS AND LINE PROFILES

For simplicity, consider only one cone (which drives one of the CO lobes), the effects of the other cone may easily be obtained by symmetry arguments and superposed (for optically thin emission) on the single-cone calculation. If we ignore the effects of hydrogen ionization or recombination and if we assume that the amount of atomic hydrogen entrained from the ambient gas is negligible, the total H I outflow rate integrated at fixed r over each cone is conserved:

$$\dot{M}_{\mathrm{H}} = 2\pi(1 - \cos\alpha) r^2 m_{\mathrm{H}}\, n_{\mathrm{H}}(r) V(r) = \text{constant}\ , \tag{A1}$$

where we have assumed that the local number density of hydrogen atoms n_{H} within each cone is a function only of r.

To find the differential H I mass, $m_{\mathrm{H}}\, n_{\mathrm{H}}\, r^2\, dr \sin\theta\, d\theta\, d\phi$, having line-of-sight velocity v, we use equation (A1) to eliminate $r^2 m_{\mathrm{H}}\, n_{\mathrm{H}}$. We then obtain

$$dM_{\mathrm{H}} = \frac{\dot{M}_{\mathrm{H}}}{2\pi(1 - \cos\alpha)\,|\,vV'(r)\,|} \sin\theta\, d\theta\, d\phi\, dv\ , \tag{A2}$$

where $V'(r) \equiv dV/dr$ is the radial derivative of the wind velocity with r being the function of (v, θ, ϕ) implicitly defined by equation (4) when $v_{\mathrm{H}} = V(r)$. Equation (A2) has been derived by considering the Jacobian of the transformation from the variables (r, θ, ϕ) to the variables (v, θ, ϕ) under the assumption that $V(r)$ is a monotonic function of r (so that the Jacobian is not singular). For optically thin emission from an angularly unresolved source, $T_A(v)dv$ is proportional to integration of equation (A2) at fixed v over all angles θ

and ϕ, i.e.,

$$T_A(v) = \frac{1}{C}\iint \frac{\dot{M}_H}{2\pi(1-\cos\alpha)|vV'(r)|}\sin\theta\, d\theta\, d\phi\ , \tag{A3}$$

where C is the constant introduced in equation (1a)

As an example, consider the power-law case, $V(r) = Ar^{-1/\beta}$, where β has a value larger than $\frac{1}{2}$ in order that the number density $n_H(r)$ obtained from equation (A1) decreases with increasing r. If we now eliminate r in favor of v, we may integrate equation (A3) to obtain equation (6) of the text:

$$T_A(v) = \frac{\dot{M}_H A^\beta}{C|v|^{2+\beta}} f(\theta_0, \alpha, \beta)\ , \tag{A4}$$

where

$$f(\theta_0, \alpha, \beta) \equiv \frac{\beta}{2\pi(1-\cos\alpha)}\int_0^{2\pi} d\phi \int_0^{\alpha} \sin\theta\, d\theta[\mathrm{sgn}\,(v)(\cos\theta_0\cos\theta + \sin\theta_0\sin\theta\cos\phi)]^{1+\beta}\ . \tag{A5}$$

In equation (A5), the cone contributes emission at negative velocities, sgn $(v) = -1$, if the combination $\cos\theta_0\cos\theta + \sin\theta_0\sin\theta\cos\phi$ is less than zero, but for unresolved measurements of a completely symmetrical biconical flow, the emission at such angles is replaced by compensating emission from the other cone. The integral in equation (A5) can be performed analytically in a number of interesting special cases. For pole-on viewing, $\theta_0 = 0$:

$$f(0, \alpha, \beta) = \frac{\beta(1-\cos^{2+\beta}\alpha)}{(2+\beta)(1-\cos\alpha)}\ . \tag{A6}$$

In the limit of a perfectly collimated beam, $\alpha \to 0$:

$$f(\theta_0, 0, \beta) = \beta\cos^{1+\beta}\theta_0\ . \tag{A7}$$

For $\beta = 1$:

$$f(\theta_0, \alpha, 1) = \frac{1}{3(1-\cos\alpha)}\left[(1-\cos^3\alpha) - \frac{3}{2}\sin^2\theta_0\cos\alpha\sin^2\alpha\right]. \tag{A8}$$

For $\beta = 2$:

$$f(\theta_0, \alpha, 2) = \frac{\cos\theta_0}{2(1-\cos\alpha)}\left[\cos^2\theta_0(1-\cos^4\alpha) + \frac{3}{2}\sin^2\theta_0\sin^4\alpha\right]. \tag{A9}$$

Similar analytic formulae can be obtained for all integral values of β.

REFERENCES

Adams, F. C., and Shu, F. H. 1986, *Ap. J.*, **308**, 836.
Bally, J. 1987, *Irish Astr. J.*, Vol. **17**, No. 3, p. 270.
Bally, J., and Stark, A., 1983, *Ap. J. (Letters)*, **266**, L61.
Bertout, C., and Magnan, C. 1987, *Astr. Ap.*, in press.
Bouvier, J., Bertout, C., Benz, W., and Mayor, M. 1986, *Astr. Ap.*, **165**, 110.
Cantó J., Dyson, J. E., and Rodríguez, L. F. 1987, in preparation.
Clark, F. O., and Laureijs, R. J. 1986, *Astr. Ap.*, **154**, L26.
Clark, F. O., Laureijs, R. J., Chiewicki, G., Zhang, C. Y., van Oesterom, W., and Kester, D. 1986, *Astr. Ap.*, **168**, L1.
Clark, F. O., and Turner, B. E. 1987, *Astr. Ap.*, **176**, 114.
Cohen, M., and Jones, B. F. 1987, *Ap. J.*, **321**, 846.
Cohen, M., and Schwartz, R. D. 1987, *Ap. J.*, **316**, 311.
Cudworth, K. M., and Herbig, G. H. 1979, *A.J.*, **84**, 548.
DeCampli, W. 1981, *Ap. J.*, **224**, 124.
DeNoyer, L. K., and Frerking, M. A. 1981, *Ap. J. (Letters)*, **246**, L37.
Draine, B. 1983, *Ap. J.*, **270**, 519.
Edwards, S., Cabrit, S., Strom, S. E., Heyer, I., and Strom, K. M. 1987, *Ap. J.*, **321**, 473.
Edwards, S., and Snell, R. L. 1984, *Ap. J.*, **281**, 237.
Edwards, S., Strom, S. E., Snell, R. L., Jarrett, T. H., Beichman, C. A., and Strom, K. M. 1986, *Ap. J. (Letters)*, **307**, L65.
Elias, J. H. 1978, *Ap. J.*, **224**, 858.
Glassgold, A. E., and Huggins, P. J. 1983, *M.N.R.A.S.*, **203**, 517.
Hartmann, L., Hewett, R., Stahler, S., and Mathieu, R. D. 1986, *Ap. J.*, **309**, 275.
Hartmann, L., and McGregor, K. B. 1981, *Ap. J.*, **242**, 260.
———. 1982, *Ap. J.*, **259**. 180.
Herbig, G. H., and Jones, B. F. 1983, *A.J.*, **88**, 1040.
Ho, P. T. P., and Barret, A. H. 1980, *Ap. J.*, **237**, 38.
Hollenbach, D., Werner, M. W., and Salpeter, E. E. 1971, *Ap. J.*, **163**, 165.
Irvine, W. M., Goldsmith, P. F., and Hjalmarson, A. 1987, in *Interstellar Processes*, ed. D. J. Hollenbach and H. A. Thronson, Jr. (Dordrecht: Reidel), p. 561.
Kutner, M. L., and Ulich, B. L. 1981, *Ap. J.*, **250**, 341.
Lada, C. J. 1985, *Ann. Rev. Astr. Ap.*, **23**, 267.
Lada, C. J., Gottlieb, C. A., Litvak, M. M., and Lilley, A. E. 1974, *Ap. J.*, **194**, 609.
Lago, M. T. V. T. 1984, *M.N.R.A.S.*, **210**, 323.
Lago, M. T. V. T., and Penston, M. V. 1982, *M.N.R.A.S.*, **198**, 429.
Levreault, R. M. 1985, Ph.D. thesis, University of Texas.
Mirabel, I. F., Cantó, J., and Rodríguez, L. F. 1983, *Rev. Mexicana Astr. Ap.*, **7**, 235.
Mirabel, I. F., Rodríguez, L. F., Cantó, J., and Arnal, E. M. 1985, *Ap. J. (Letters)*, **294**, L39.
Mundt, R. 1984, in *Protostars and Planets II, The University of Arizona Press*, ed. D. C. Black and M. S. Mattews (Tucson: University of Arizona Press), p. 414.
Pudritz, R. E., and Norman, C. A. 1983, *Ap. J.*, **274**, 677.
———. 1986, *Ap. J.*, **301**, 571.
Rodríguez, L. F., and Cantó, J. 1983, *Rev. Mexicana Astr. Ap.*, **8**, 163.
Rudolph, A., and Welch, W. J. 1988, *Ap. J. (Letters)*, **326**, L31.
Shu, F. H., Adams, F. C., and Lizano, S. 1987, *Ann. Rev. Astr. Ap.*, **25**, 23.
Shu, F. H., and Terebey, S. 1984, in *Cool Stars, Stellar Systems, and the Sun*, ed. S. Baliunas and L. Hartmann (Berlin: Springer-Verlag), p. 78.
Snell, R. L., Bally, J., Strom, S. E., and Strom, K. M. 1985, *Ap. J.*, **290**, 587.
Snell, R. L., and Edwards, S. 1981, *Ap. J.*, **251**, 103.

Snell, R. L., Loren, R. B., and Plambeck, R. L. 1980, *Ap. J. (Letters)*, **239**, L17.
Snell, R. L., and Schloerb, F. B. 1985, *Ap. J.*, **295**, 490.
Snell, R. L., Scoville, N. Z., Sanders, D. B., and Erickson, N. R. 1984, *Ap. J.*, **284**, 176.
Strom, K. M., Strom, S. E., Wolf, S. C., Morgan, J., and Wenz, M. 1986, *Ap. J. Suppl.*, **62**, 39.
Strom, S. E., Grasdalen, G. L., and Strom, K. M. 1974, *Ap. J.*, **191**, 111.
Strom, S. E., Vrba, F. J., and Strom, K. M. 1976, *A.J.*, **81**, 314.
Uchida, Y., and Shibata, K. 1985, *Pub. Astr. Soc. Japan*, **37**, 515.
Vogel, S., and Kuhi, L. 1981, *Ap. J.*, **245**, 960.
Vogel, S. N., Wright, M. C. H., Plambeck, R. L., and Welch, W. J. 1984, *Ap. J.*, **283**, 655.
Walmsley, C. M., and Menten, K. M. 1987, *Astr. Ap.*, in press.

TETSUO HASEGAWA and SAEKO HAYASHI: Tokyo Astronomical Observatory, University of Tokyo, Tokyo, Japan

CARL HEILES, BON-CHUL KOO, SUSANA LIZANO, and FRANK H. SHU: Astronomy Department, University of California, Berkeley, CA 94720

I. FELIX MIRABEL: Department of Physics, Faculty of Natural Science, University of Puerto Rico, Rio Piedras Campus, Rio Piedras, PR 00931

LUIS F. RODRÍGUEZ: Instituto de Astronomia, Apdo. Postal 70-264, UNAM, 04510 Mexico D.F., Mexico